High-order kernels for Riemannian Wavefield Extrapolation

Paul Sava (Colorado School of Mines)
Sergey Fomel (University of Texas at Austin)[1]

ABSTRACT

Riemannian wavefield extrapolation (RWE) is a technique for one-way extrapolation of acoustic waves. RWE generalizes wavefield extrapolation by downward continuation by considering coordinate systems different from conventional Cartesian. Coordinate systems can conform with the extrapolated wavefield, with the velocity model or with the acquisition geometry.
When coordinate systems conform with the propagated wavefield, extrapolation can be done accurately using low-order kernels. However, in complex media or in cases the coordinate systems do not conform with the propagating wavefields, low order kernels are not accurate enough and need to be replaced by more accurate, higher order kernels. Since RWE is based on factorization of an acoustic wave-equation, higher order kernels can be constructed using methods analogous with the one employed for factorization of the acoustic wave-equation in Cartesian coordinates. Thus, we can construct space-domain finite-differences as well as mixed-domain techniques for extrapolation.
High-order RWE kernels improve the accuracy of extrapolation, particularly when the Riemannian coordinate systems does not match closely the general direction of wave propagation.

INTRODUCTION

Riemannian wavefield extrapolation (Sava and Fomel, 2005) generalizes solutions to the Helmholtz equation in general Riemannian coordinate systems. Conventionally, the Helmholtz equation is solved in Cartesian coordinates which represent special cases of Riemannian coordinates. The main requirements imposed on the Riemannian coordinate systems are that they maintain orthogonality between the extrapolation coordinate and the other coordinates (2 in 3D, 1 in 2D). This requirement can be relaxed when using an even more general form of RWE in non-orthogonal coordinates (Shragge, 2007). In addition, it is desirable that the coordinate system does not triplicate, although numerical methods can stabilize extrapolation even in such situations (Sava and Fomel, 2005). Thus, wavefield extrapolation in Riemannian coordinates has the flexibility to be used in many applications where those basic conditions are

[1]**e-mail:** psava@mines.edu, sergey.fomel@beg.utexas.edu

fulfilled. Cartesian coordinate systems, including tilted coordinates, are special cases of Riemannian coordinate systems.

Two straightforward applications of wave propagation in Riemannian coordinates are extrapolation in a coordinate system created by ray tracing in a smooth background velocity (Sava and Fomel, 2005), and extrapolation with a coordinate system created by conformal mapping of a given geometry to a regular space, for example migration from topography (Shragge and Sava, 2005).

Coordinate systems created by ray tracing in a background medium often well represent wavefield propagation. In this context, we effectively split wave propagation effects into two parts: one part accounting for the general trend of wave propagation, which is incorporated in the coordinate system, and the other part accounting for the details of wavefield scattering due to rapid velocity variations. If the background medium is close to the real one, the wave-propagation can be properly described with low-order operators. However, if the background medium is far from the true one, the wavefield departs from the general direction of the coordinate system and the low-order extrapolators are not enough for accurate description of wave propagation.

For coordinate system describing a geometrical property of the medium (e.g. migration from topography), there is no guarantee that waves propagate in the direction of extrapolation. This situation is similar to that of Cartesian coordinates when waves propagate away from the vertical direction, except that conformal mapping gives us the flexibility to define any coordinates, as required by acquisition. In this case, too, low-order extrapolators are not enough for accurate description of wave propagation.

Therefore, there is need for higher-order Riemannian wavefield extrapolators in order to handle correctly waves propagating obliquely relative to the coordinate system. Usually, the high-order extrapolators are implemented as mixed operators, part in the Fourier domain using a reference medium, part in the space domain as a correction from the reference medium. Many methods have been developed for high-order extrapolation in Cartesian coordinates. In this paper, we explore some of those extrapolators in Riemannian coordinates, in particular high-order finite-differences solutions (Claerbout, 1985), and methods from the pseudo-screen family (Huang et al., 1999) and Fourier finite-differences family (Ristow and Ruhl, 1994; Biondi, 2002). In theory, any other high-order extrapolator developed in Cartesian coordinates can have a correspondent in Riemannian coordinates.

In this paper, we implement the finite-differences portion of the high-order extrapolators with implicit methods. Such solutions are accurate and robust, but they face difficulties for 3D implementations because the finite-differences part cannot be solved by fast tridiagonal solvers anymore and require more complex and costlier approaches (Claerbout, 1998; Rickett et al., 1998). The problem of 3D wavefield extrapolation is addressed in Cartesian coordinates either by splitting the one-way wave-equation along orthogonal directions (Ristow and Ruhl, 1997), or by explicit numerical solutions (Hale, 1991). Similar approaches can be employed for 3D Riemannian extrapolation. The explicit solution seems more appropriate, since splitting

is difficult due to the mixed terms of the Riemannian equations. In this paper, we concentrate our attention to higher-order kernels implemented with implicit methods.

RIEMANNIAN WAVEFIELD EXTRAPOLATION

Riemannian wavefield extrapolation (Sava and Fomel, 2005) generalizes solutions to the Helmholtz equation of the acoustic wave-equation

$$\Delta \mathcal{U} = -\omega^2 s^2 \mathcal{U} \ , \tag{1}$$

to coordinate systems that are different from simple Cartesian, where extrapolation is performed strictly in the downward direction. In equation (1), s is slowness, ω is temporal frequency, and $\mathcal{U}$ is a monochromatic acoustic wave. The Laplacian operator Δ takes different forms according to the coordinate system used for discretization.

Assume that we describe the physical space in Cartesian coordinates x, y and z, and that we describe a Riemannian coordinate system using coordinates ξ, η and ζ. The two coordinate systems are related through a mapping

$$x = x(\xi,\eta,\zeta) \tag{2}$$
$$y = y(\xi,\eta,\zeta) \tag{3}$$
$$z = z(\xi,\eta,\zeta) \tag{4}$$

which allows us to compute derivatives of the Cartesian coordinates relative to the Riemannian coordinates.

A special case of the mapping (2)-(4) is defined when the Riemannian coordinate system is constructed by ray tracing. The coordinate system is defined by traveltime τ and shooting angles, for example. Such coordinate systems have the property that they are semi-orthogonal, i.e. one axis is orthogonal on the other two, although the later axes are not necessarily orthogonal on one-another.

Following the derivation in Sava and Fomel (2005), the acoustic wave-equation in Riemannian coordinates can be written as:

$$c_{\zeta\zeta}\frac{\partial^2 \mathcal{U}}{\partial \zeta^2} + c_{\xi\xi}\frac{\partial^2 \mathcal{U}}{\partial \xi^2} + c_{\eta\eta}\frac{\partial^2 \mathcal{U}}{\partial \eta^2} + c_{\zeta}\frac{\partial \mathcal{U}}{\partial \zeta} + c_{\xi}\frac{\partial \mathcal{U}}{\partial \xi} + c_{\eta}\frac{\partial \mathcal{U}}{\partial \eta} + c_{\xi\eta}\frac{\partial^2 \mathcal{U}}{\partial \xi \partial \eta} = -\left(\omega s\right)^2 \mathcal{U} \ , \tag{5}$$

where coefficients c_{ij} are functions of the coordinate system and can be computed numerically for any given coordinate system mapping (2)-(4).

The acoustic wave-equation in Riemannian coordinates (5) contains both first and second order terms, in contrast with the normal Cartesian acoustic wave-equation which contains only second order terms. We can construct an approximate Riemannian wavefield extrapolation method by dropping the first-order terms in equation (5). This approximation is justified by the fact that, according to the theory of characteristics for second-order hyperbolic equations (Courant and Hilbert, 1989), the first-order

terms affect only the amplitude of the propagating waves. To preserve the kinematics, it is sufficient to retain only the second order terms of equation (5):

$$c_{\zeta\zeta}\frac{\partial^2 \mathcal{U}}{\partial \zeta^2} + c_{\xi\xi}\frac{\partial^2 \mathcal{U}}{\partial \xi^2} + c_{\eta\eta}\frac{\partial^2 \mathcal{U}}{\partial \eta^2} + c_{\xi\eta}\frac{\partial^2 \mathcal{U}}{\partial \xi \partial \eta} = -\left(\omega s\right)^2 \mathcal{U} \; . \tag{6}$$

From equation (6) we can derive the following dispersion relation of the acoustic wave-equation in Riemannian coordinates

$$-c_{\zeta\zeta}k_\zeta^2 - c_{\xi\xi}k_\xi^2 - c_{\eta\eta}k_\eta^2 - c_{\xi\eta}k_\xi k_\eta = -\left(\omega s\right)^2 \; , \tag{7}$$

where k_ζ, k_ξ and k_η are wavenumbers associated with the Riemannian coordinates ζ, ξ and η. Coefficients $c_{\xi\xi}$, $c_{\eta\eta}$ and $c_{\zeta\zeta}$ are known quantities defined using the coordinate system mapping (2)-(4). For one-way wavefield extrapolation, we need to solve the quadratic equation (7) for the wavenumber of the extrapolation direction k_ζ, and select the solution with the appropriate sign for the desired extrapolation direction:

$$k_\zeta = \sqrt{\frac{\left(\omega s\right)^2}{c_{\zeta\zeta}} - \frac{c_{\xi\xi}}{c_{\zeta\zeta}}k_\xi^2 - \frac{c_{\eta\eta}}{c_{\zeta\zeta}}k_\eta^2 - \frac{c_{\xi\eta}}{c_{\zeta\zeta}}k_\xi k_\eta} \; . \tag{8}$$

The 2D equivalent of equation (8) takes the form:

$$k_\zeta = \sqrt{\frac{\left(\omega s\right)^2}{c_{\zeta\zeta}} - \frac{c_{\xi\xi}}{c_{\zeta\zeta}}k_\xi^2} \; . \tag{9}$$

In ray coordinates, defined by $\zeta \equiv \tau$ (propagation time) and $\xi \equiv \gamma$ (shooting angle), we can re-write equation (9) as

$$k_\tau = \sqrt{\left(\omega s \alpha\right)^2 - \left(\frac{\alpha}{J}k_\gamma\right)^2} \; , \tag{10}$$

where α represents velocity and J represents geometrical spreading. The quantities α and J characterize the extrapolation coordinate system: α describes the velocity used for construction of ray coordinate system; J describes the spreading or focusing of the coordinate system. In general, the velocity used for construction of the coordinate system is different from the velocity used for extrapolation, as suggested by Sava and Fomel (2005) and illustrated later in this paper.

We can further simplify the computations by introducing the notation

$$a = s\alpha \; , \tag{11}$$

$$b = \frac{\alpha}{J} \; , \tag{12}$$

thus equation (10) taking the form

$$k_\tau = \sqrt{\left(\omega a\right)^2 - \left(b k_\gamma\right)^2} \; . \tag{13}$$

For Cartesian coordinate systems, $\alpha = 1$ and $J = 1$, equation (13) reduces to the known dispersion relation

$$k_z = \sqrt{\omega^2 s^2 - k_x^2} \; , \tag{14}$$

where k_z and k_x are depth and position extrapolation wavenumbers.

EXTRAPOLATION KERNELS

Extrapolation using equation (13) implies that the coefficients defining the problem, a and b, are not changing spatially. In this case, we can perform extrapolation using a simple phase-shift operation

$$\mathcal{U}_{\tau+\Delta\tau} = \mathcal{U}_\tau e^{ik_\tau \Delta\tau} \;, \tag{15}$$

where $\mathcal{U}_{\tau+\Delta\tau}$ and $\mathcal{U}_\tau$ represent the acoustic wavefield at two successive extrapolation steps, and k_τ is the extrapolation wavenumber defined by equation (13).

For media with lateral variability of the coefficients a and b, due to either velocity variation or focusing/defocusing of the coordinate system, we cannot use in extrapolation the wavenumber computed directly using equation (13). Like for the case of extrapolation in Cartesian coordinates, we need to approximate the wavenumber k_τ using expansions relative to a and b. Such approximations can be implemented in the space-domain, in the Fourier domain or in mixed space-Fourier domains.

Space-domain extrapolation

The space-domain finite-differences solution to equation (13) is derived based on a square-root expansion as suggested by Francis Muir (Claerbout, 1985):

$$k_\tau \approx \omega a + \omega \frac{\nu \left(\frac{k_\gamma}{\omega}\right)^2}{\mu - \rho \left(\frac{k_\gamma}{\omega}\right)^2} \;, \tag{16}$$

where the coefficients μ, ν and ρ take the form derived in Appendix A:

$$\nu = -c_1 a \left(\frac{b}{a}\right)^2 \;, \tag{17}$$

$$\mu = 1 \;, \tag{18}$$

$$\rho = c_2 \left(\frac{b}{a}\right)^2 \;. \tag{19}$$

In the special case of Cartesian coordinates, $a = s$ and $b = 1$, equation (16) takes the familiar form

$$k_\tau \approx \omega s - \omega \frac{\frac{c_1}{s} \left(\frac{k_\gamma}{\omega}\right)^2}{1 - \frac{c_2}{s^2} \left(\frac{k_\gamma}{\omega}\right)^2} \;, \tag{20}$$

where the coefficients c_1 and c_2 take different values for different orders of Muir's expansion: $(c_1, c_2) = (0.50, 0.00)$ for the 15° equation, and $(c_1, c_2) = (0.50, 0.25)$ for the 45° equation, etc. For extrapolation in Riemannian coordinates, the meaning of 15°, 45° etc is not defined. We use this terminology here to indicate orders of accuracy comparable to the ones defined in Cartesian coordinates.

Mixed-domain extrapolation

Mixed-domain solutions to the one-way wave equation consist of decompositions of the extrapolation wavenumber defined in equation (13) in terms computed in the Fourier domain for a reference of the extrapolation medium, followed by a finite-differences correction applied in the space-domain. For equation (13), a generic mixed-domain solution has the form:

$$k_\tau \approx k_{\tau 0} + \omega\,(a - a_0) + \omega \frac{\nu \left(\frac{k_\gamma}{\omega}\right)^2}{\mu - \rho \left(\frac{k_\gamma}{\omega}\right)^2}\ , \tag{21}$$

where a_0 and b_0 are reference values for the medium characterized by the parameters a and b, and the coefficients μ, ν and ρ take different forms according to the type of approximation. As for usual Cartesian coordinates, $k_{\tau 0}$ is applied in the Fourier domain, and the other two terms are applied in the space domain. If we limit the space-domain correction to the thin lens term, $\omega\,(a - a_0)$, we obtain the equivalent of the split-step Fourier (SSF) method (Stoffa et al., 1990) in Riemannian coordinates.

Appendix A details the derivations for two types of expansions known by the names of pseudo-screen (Huang et al., 1999), and Fourier finite-differences (Ristow and Ruhl, 1994; Biondi, 2002). Other extrapolation approximations are possible, but are not described here, for simplicity.

- **Pseudo-screen method:**

  The coefficients for the pseudo-screen approximation to equation (21) are

$$\nu = a_0 \left[c_1 \left(\frac{a}{a_0} - 1 \right) - \left(\frac{b}{b_0} - 1 \right) \right] \left(\frac{b_0}{a_0} \right)^2\ , \tag{22}$$

$$\mu = 1\ , \tag{23}$$

$$\rho = 3 c_2 \left(\frac{b_0}{a_0} \right)^2\ , \tag{24}$$

  where a_0 and b_0 are reference values for the medium characterized by parameters a and b. In the special case of Cartesian coordinates, $a = s$ and $b = 1$, equation (21) with coefficients equation (22) takes the familiar form

$$k_\tau \approx k_{\tau 0} + \omega \left[1 + \frac{\frac{c_1}{s_0^2} \left(\frac{k_\gamma}{\omega}\right)^2}{1 - \frac{3 c_2}{s_0^2} \left(\frac{k_\gamma}{\omega}\right)^2} \right] (s - s_0)\ , \tag{25}$$

  where the coefficients c_1 and c_2 take different values for different orders of the finite-differences term: $(c_1, c_2) = (0.50, 0.00)$, $(c_1, c_2) = (0.50, 0.25)$, etc. When $(c_1, c_2) = (0.00, 0.00)$ we obtain the usual split-step Fourier equation (Stoffa et al., 1990).

- **Fourier finite-differences method:**

  The coefficients for the Fourier finite-differences solution to equation (21) are

$$\nu = \frac{1}{2}\delta_1^2 \,, \tag{26}$$

$$\mu = \delta_1 \,, \tag{27}$$

$$\rho = \frac{1}{4}\delta_2 \,, \tag{28}$$

  where, by definition,

$$\delta_1 = a\left(\frac{b}{a}\right)^2 - a_0\left(\frac{b_0}{a_0}\right)^2 \,, \tag{29}$$

$$\delta_2 = a\left(\frac{b}{a}\right)^4 - a_0\left(\frac{b_0}{a_0}\right)^4 \,. \tag{30}$$

  a_0 and b_0 are reference values for the medium characterized by the parameters a and b. In the special case of Cartesian coordinates, $a = s$ and $b = 1$, equation (21) with coefficients equation (26) takes the familiar form:

$$k_\tau \approx k_{\tau 0} + \omega\left[1 + \frac{\frac{c_1}{ss_0}\left(\frac{k_\gamma}{\omega}\right)^2}{1 - c_2\left(\frac{1}{s^2} + \frac{1}{ss_0} + \frac{1}{s_0^2}\right)\left(\frac{k_\gamma}{\omega}\right)^2}\right](s - s_0) \,, \tag{31}$$

  where the coefficients c_1 and c_2 take different values for different orders of the finite-differences term: $(c_1, c_2) = (0.50, 0.00)$ for 15°, $(c_1, c_2) = (0.50, 0.25)$ for 45°, etc. When $c_1 = c_2 = 0.0$ we obtain the usual split-step Fourier equation (Stoffa et al., 1990).

EXAMPLES

We illustrate the higher-order RWE extrapolators with impulse responses for two synthetic models.

The first example is based on the Marmousi model (Versteeg, 1994). We construct the coordinate system by ray tracing from a point source at the surface in a smooth version of the real velocity model. Figure 1 shows the velocity model with the coordinate system overlaid, and Figures 2(a)-2(b) show the coordinate system coefficients a and b defined in equations (11) and (12).

The goal of this test model is to illustrate the higher-order extrapolation kernels in a fairly complex model using a simple coordinate system. In this way, the coordinate system and the real direction of wave propagation depart from one-another, thus accurate extrapolation requires higher order kernels. The coordinate system is

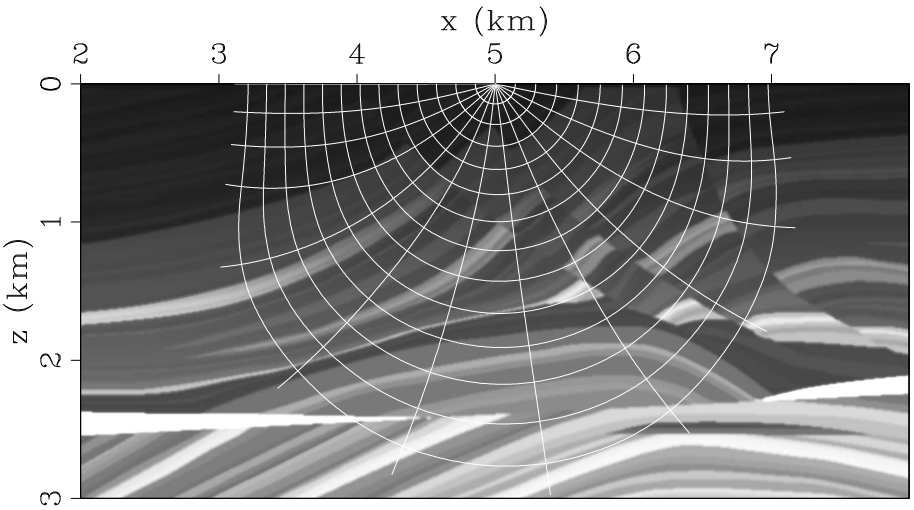

Figure 1: Velocity map and Riemannian coordinate system for the Marmousi example.

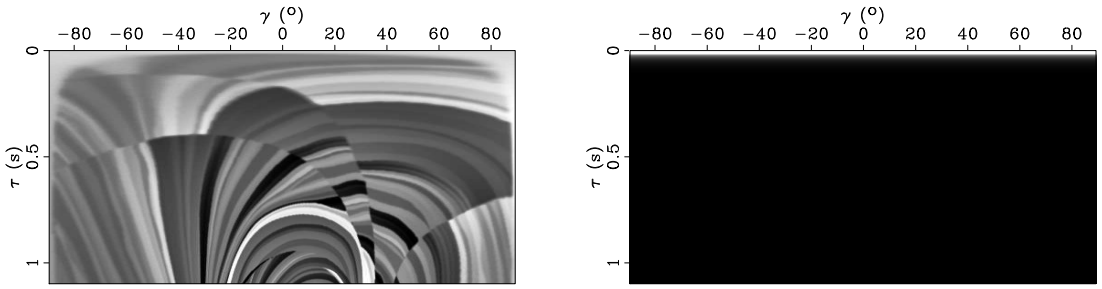

(a) (b)

Figure 2: Coordinate system coefficients defined in equations (11) and (12). (a) Parameter $a = s\alpha$ in ray coordinates. (b) Parameter $b = \alpha/J$ in ray coordinates.

constructed from a point at the location of the wave source. This setting is similar to the case of extrapolation from a point source in Cartesian coordinates, where high-angle [2] propagation requires high-order kernels.

Figures 3(a)-3(d) show impulse responses for a point source computed with various extrapolators in ray coordinates (τ and γ). Panels (a) and (c) show extrapolation with the 15° and 60°, respectively. Panels (b) and (d) show extrapolation with the pseudo-screen (PSC) equation, and the Fourier finite-differences (FFD) equation, respectively. All plots are displayed in ray coordinates. We can observe that the angular accuracy of the extrapolator improves for the more accurate extrapolators. The finite-differences solutions (panels a and c) show the typical behavior of such solutions for the 15° and 60° equations (e.g. the cardioid for 60°), but in the more general setting of Riemannian extrapolation. The mixed-domain extrapolators (panels b and d) are more accurate the finite-differences extrapolators. The main differences occur at the highest propagation angles. As for the case of Cartesian extrapolation, the most accurate kernel of those compared is the equivalent of Fourier finite-differences.

Figures 4(a)-4(d) show the corresponding plots in Figures 3(a)-3(d) mapped in the physical coordinates. The overlay is an outline of the extrapolation coordinate system. After re-mapping to the physical space, the comparison of high-angle accuracy for the various extrapolators is more apparent, since it now has physical meaning.

Figures 5(a)-5(b) show a side-by-side comparison of equivalent extrapolators in Riemannian and Cartesian coordinates. The impulse response in Figure 5(a) shows the limits of Cartesian extrapolation in propagating waves correctly up to 90°. The Riemannian extrapolator in Figure 5(b) handles much better waves propagating at high angles, including energy that is propagating upward relative to the physical coordinates.

The second example is based on a model with a large lateral gradient which makes an incident plane wave overturn. A small Gaussian anomaly, not used in the construction of the coordinate system, forces the propagating wave to triplicate and move at high angles relative to the extrapolation direction. Figure 6 shows the velocity model with the coordinate system overlaid. Figures 7(a)-7(b) show the coordinate system coefficients, a and b defined in equations (11) and (12).

The goal of this model is to illustrate Riemannian wavefield extrapolation in a situation which cannot be handled correctly by Cartesian extrapolation, no matter how accurate an extrapolator we use. In this example, an incident plane wave is overturning, thus becoming evanescent for the solution constructed in Cartesian coordinates. Furthermore, the Gaussian anomaly shown in Figure 7(a) causes wavefield triplication, thus requiring high-order kernels for the Riemannian extrapolator.

Figures 8(a)-8(d) show impulse responses for an incident plane wave computed

[2]If the extrapolation axis is time, the meaning of higher angle accuracy is not well defined. We can use this terminology to associate the mathematical meaning of the approximation for the square-root by analogy with the Cartesian equivalents.

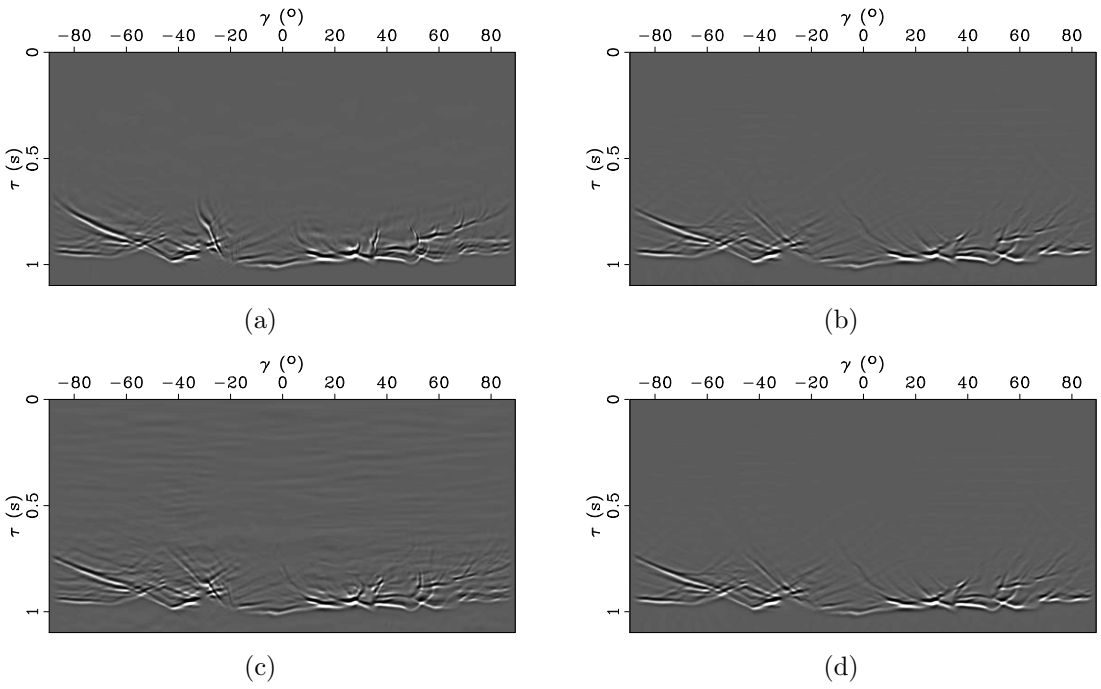

Figure 3: Migration impulse responses in Riemannian coordinates. (a) Extrapolation with the 15° finite-differences equation. (c) Extrapolation with the 60° finite-differences equation. (b) Extrapolation with the pseudo-screen (PSC) equation. (d) Extrapolation with the Fourier finite-differences (FFD) equation.

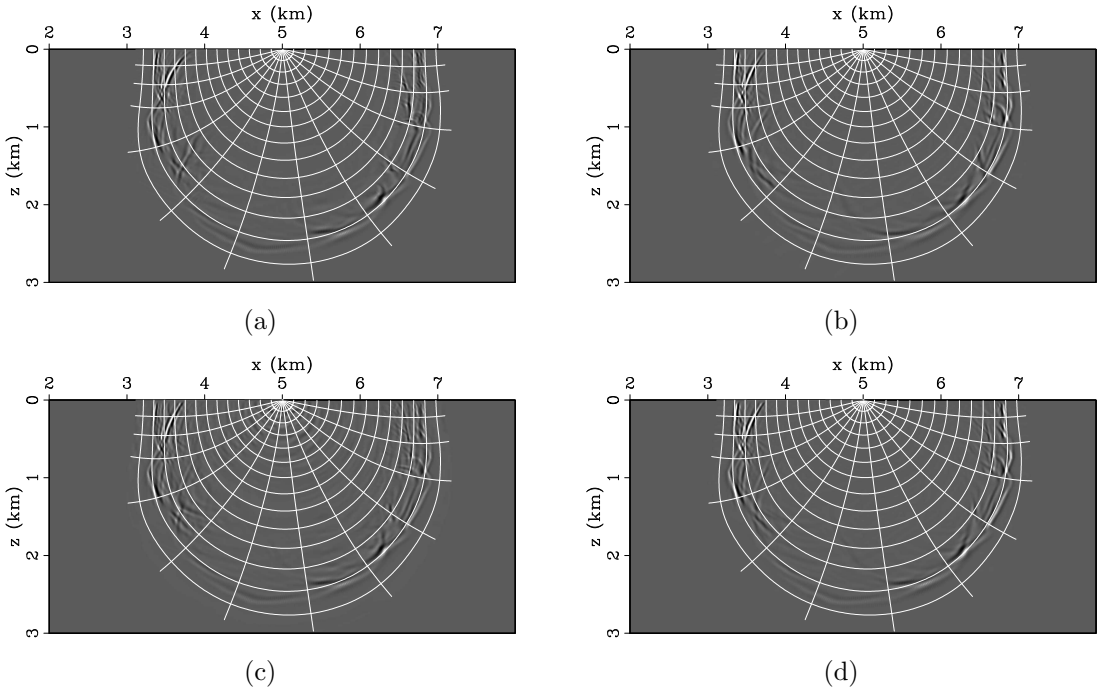

Figure 4: Migration impulse responses in Riemannian coordinates after mapping to Cartesian coordinates. (a) Extrapolation with the 15° finite-differences equation. (c) Extrapolation with the 60° finite-differences equation. (b) Extrapolation with the pseudo-screen (PSC) equation. (d) Extrapolation with the Fourier finite-differences (FFD) equation.

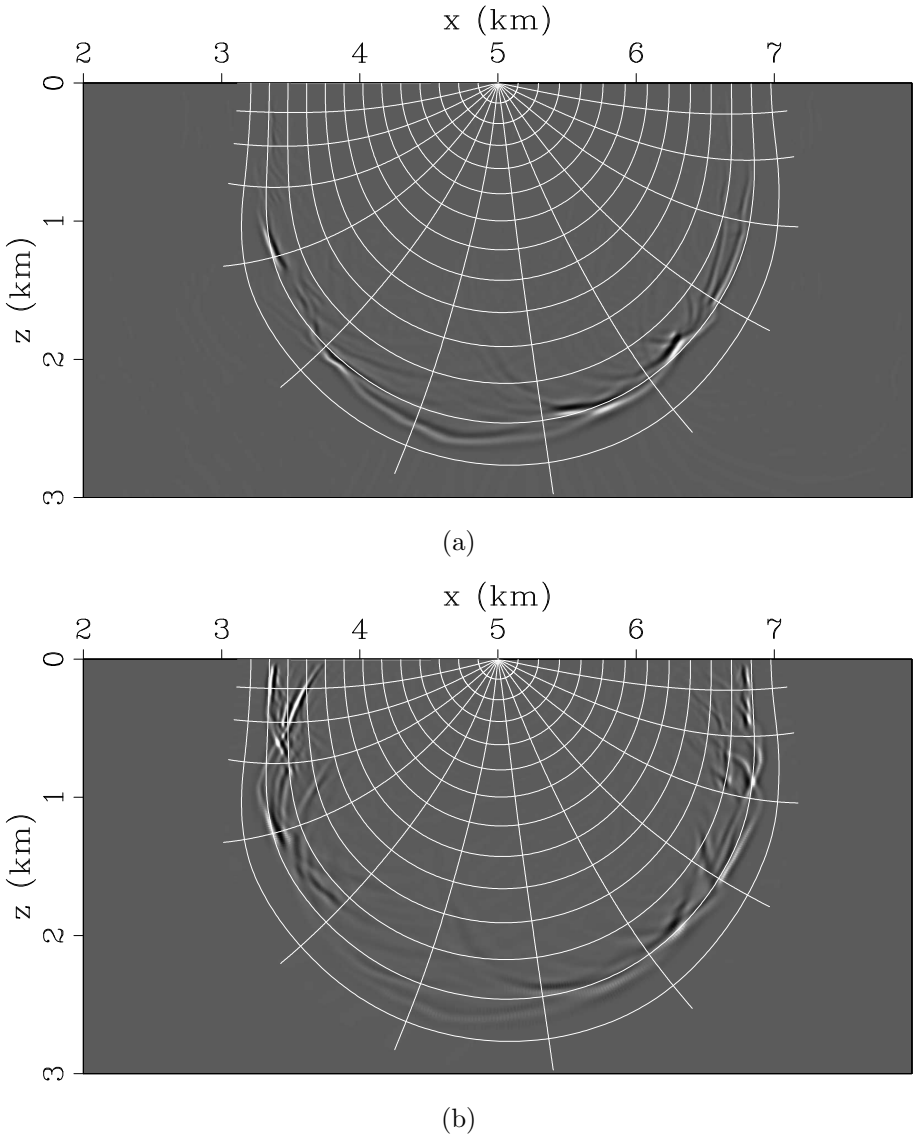

Figure 5: Comparison of extrapolation in Cartesian and Riemannian coordinates. (a) Split-step Fourier extrapolation in Cartesian coordinates. (b) Split-step Fourier extrapolation in Riemannian coordinates.

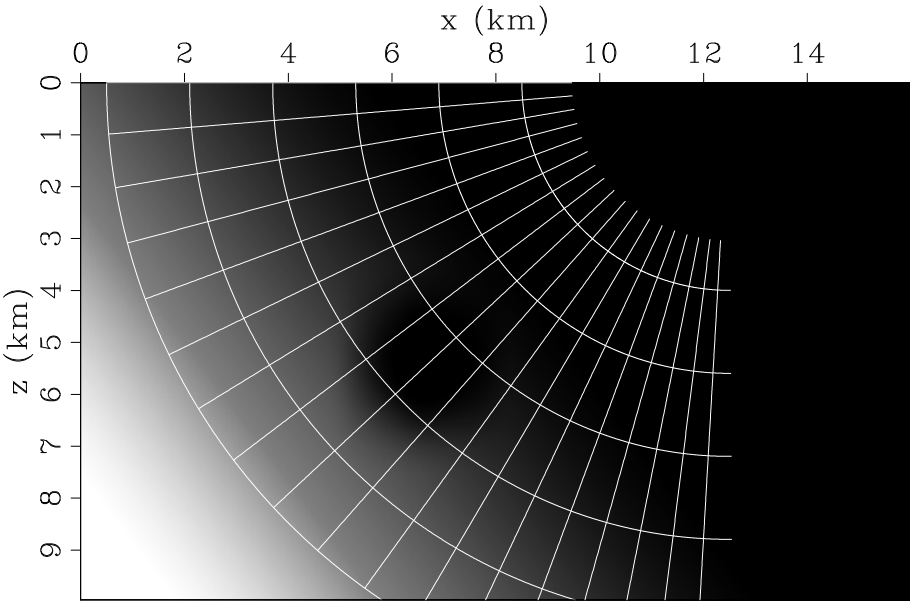

Figure 6: Velocity map and Riemannian coordinate system for the large-gradient model experiment.

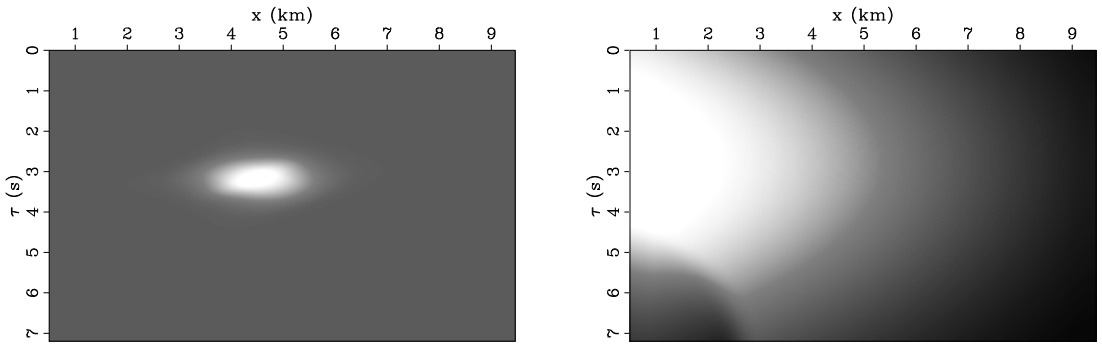

(a) (b)

Figure 7: Coordinate system coefficients defined in equations (11) and (12). (a) Parameter $a = s\alpha$ in ray coordinates. (b) Parameter $b = \alpha/J$ in ray coordinates.

with various extrapolators in ray coordinates (τ and γ). Panels (a) and (c) show extrapolation with the 15° and 60° finite-differences equations, respectively. Panel (b) and (d) show extrapolation with the pseudo-screen (PSC) equation and the Fourier finite-differences (FFD) equation, respectively. All plots are displayed in ray coordinates. As for the preceding example, we observe higher angular accuracy as we increase the order of the extrapolator. The equivalent FFD extrapolator shows the highest accuracy of all tested extrapolators.

As in the preceding example, Figures 9(a)-9(d) show the corresponding plots in Figures 8(a)-8(d) mapped in the physical coordinates. The overlay is an outline of the extrapolation coordinate system.

Finally, figures 10(a) and 10(b) show a side-by-side comparison of equivalent extrapolators in Riemannian and Cartesian coordinates. The impulse response in Figure 10(a) clearly shows the failure of the Cartesian extrapolator in propagating waves correctly even up to 90°. The Riemannian extrapolator in Figure 10(b) handles much better overturning waves, including energy that is propagating upward relative to the vertical direction.

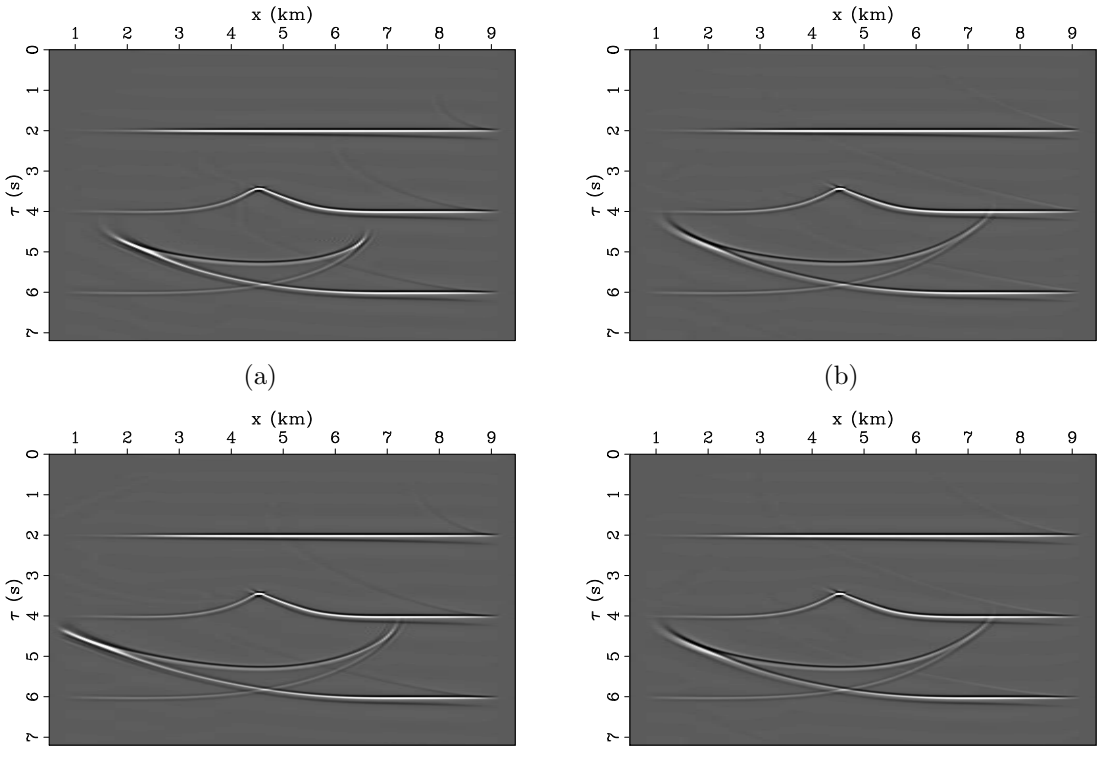

Figure 8: Migration impulse responses in Riemannian coordinates. (a) Extrapolation with the 15° finite-differences equation. (c) Extrapolation with the 60° finite-differences equation. (b) Extrapolation with the pseudo-screen (PSC) equation. (d) Extrapolation with the Fourier finite-differences (FFD) equation.

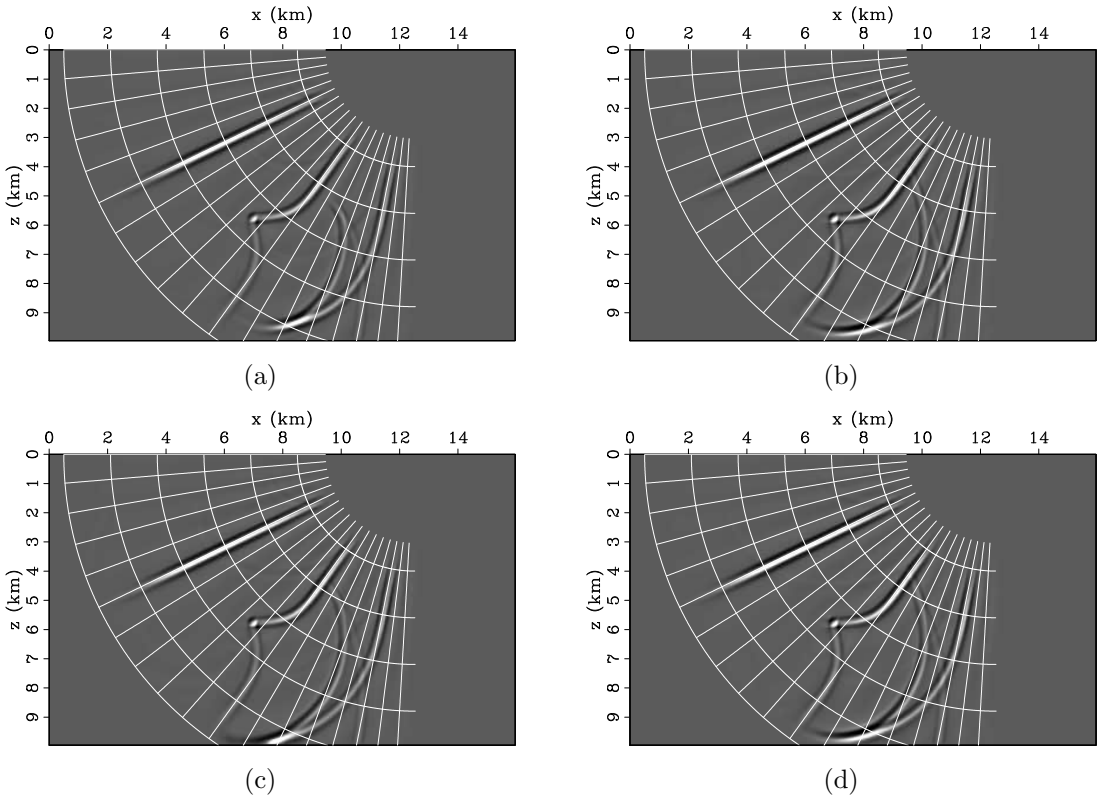

Figure 9: Migration impulse responses in Riemannian coordinates after mapping to Cartesian coordinates. (a) Extrapolation with the 15° finite-differences equation. (c) Extrapolation with the 60° finite-differences equation. (b) Extrapolation with the pseudo-screen (PSC) equation. (d) Extrapolation with the Fourier finite-differences (FFD) equation.

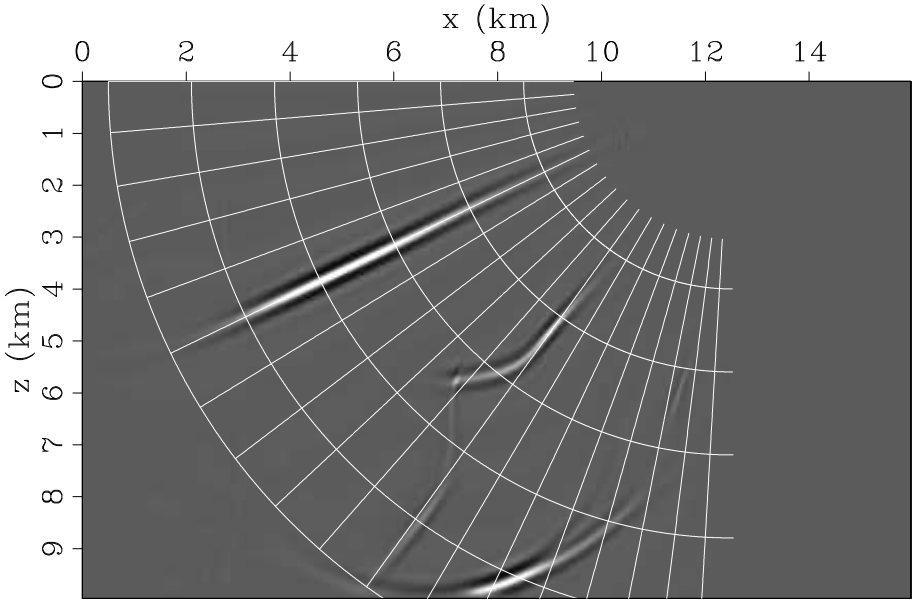

(a)

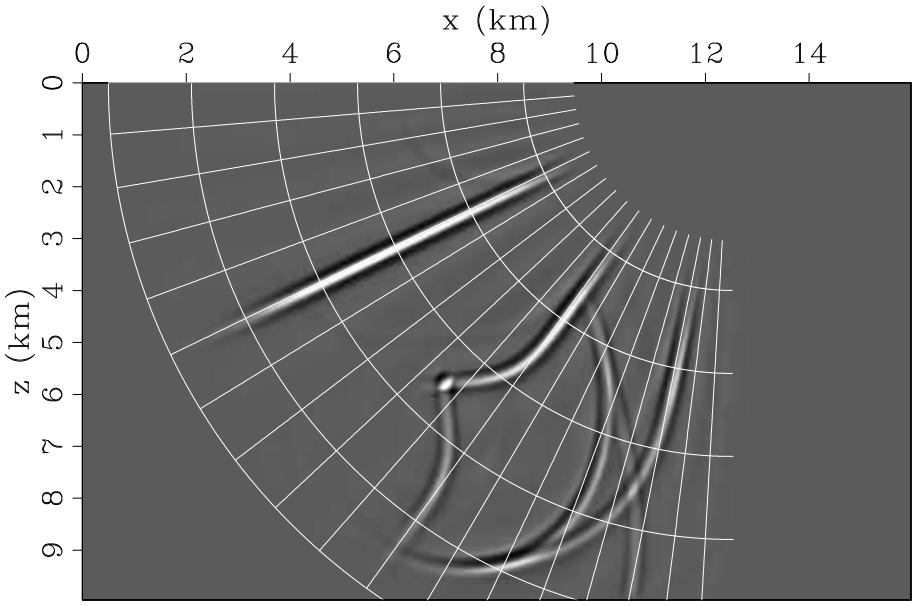

(b)

Figure 10: Comparison of extrapolation in Cartesian and Riemannian coordinates. (a) Split-step Fourier extrapolation in Cartesian coordinates. (b) Split-step Fourier extrapolation in Riemannian coordinates.

DISCUSSION

Accurate wave-equation migration using Riemannian wavefield extrapolation requires a choice of coordinate system that exploits its higher extrapolation accuracy. An effective choice of coordinate system would be one that minimizes the difference between the extrapolation direction and the direction of wave propagation. If this condition is fulfilled, we can achieve high-angle accuracy using low-order extrapolation kernels. Otherwise, we need to extrapolate seismic wavefields with high-order kernels, like the ones described in this paper.

Shot-record migration requires selection of coordinate systems for the source and receiver wavefields. Optimal selection of coordinate systems in this situation is not a trivial task, since the source and receiver wavefields are optimally described by different coordinate systems which also vary with location. However, if we employ high-order extrapolation kernels, different seismic experiments may share the same approximately optimal coordinate system. An easy way to illustrate this idea is represented by imaging in (tilted) Cartesian coordinate systems, which are just special cases of Riemannian coordinates (Sava and Fomel, 2006). A complete treatment of this topic remains subject for future research.

CONCLUSIONS

Higher-order Riemannian wavefield extrapolation is needed when the coordinate system does not closely conform with the general direction of wavefield propagation. This situation occurs, for example, when the coordinate system is created by ray tracing in a medium that is different from the one used for extrapolation, or when the coordinate system is constructed based on geometrical properties of the acquisition geometry (e.g. migration from topography). Space-domain and mixed-domain finite-difference solutions to Riemannian wavefield extrapolation improve the angular accuracy. 3D solutions can be addressed with explicit finite-differences or by using splitting and implicit methods, similarly with the techniques used for Cartesian extrapolation.

ACKNOWLEDGMENT

ExxonMobil provided partial financial support of this research.

APPENDIX A

SPACE-DOMAIN FINITE-DIFFERENCES

Starting from equation (13), based on the Muir expansion for the square-root (Claerbout, 1985), we can write successively:

$$k_\tau = \omega a \sqrt{1-\left(\frac{bk_\gamma}{a\omega}\right)^2} \tag{A-1}$$

$$\approx \omega a \left[1-\frac{c_1\left(\frac{bk_\gamma}{a\omega}\right)^2}{1-c_2\left(\frac{bk_\gamma}{a\omega}\right)^2}\right] \tag{A-2}$$

$$\approx \omega a - \omega \frac{c_1 a \left(\frac{b}{a}\right)^2 \left(\frac{k_\gamma}{\omega}\right)^2}{1-c_2\left(\frac{b}{a}\right)^2\left(\frac{k_\gamma}{\omega}\right)^2} \; . \tag{A-3}$$

If we make the notations

$$\nu = -c_1 a \left(\frac{b}{a}\right)^2 \; , \tag{A-4}$$

$$\mu = 1 \; , \tag{A-5}$$

$$\rho = c_2 \left(\frac{b}{a}\right)^2 \; . \tag{A-6}$$

we obtain the finite-differences solution to the one-way wave equation in Riemannian coordinates:

$$k_\tau \approx \omega a + \omega \frac{\nu\left(\frac{k_\gamma}{\omega}\right)^2}{\mu-\rho\left(\frac{k_\gamma}{\omega}\right)^2} \; . \tag{A-7}$$

MIXED DOMAIN — PSEUDO-SCREEN

The pseudo-screen solution to equation (13) derives from a first-order expansion of the square-root around a_0 and b_0 which are reference values for the medium characterized by the parameters a and b:

$$k_\tau \approx k_{\tau 0} + \left.\frac{\partial k_\tau}{\partial a}\right|_{a_0,b_0} (a-a_0) + \left.\frac{\partial k_\tau}{\partial b}\right|_{a_0,b_0} (b-b_0) \; . \tag{A-8}$$

The partial derivatives relative to a and b, respectively, are:

$$\left.\frac{\partial k_\tau}{\partial a}\right|_{a_0,b_0} = \omega \frac{1}{\sqrt{1-\left(\frac{b_0 k_\gamma}{a_0\omega}\right)^2}} \approx \omega \left[1+\frac{c_1\left(\frac{b_0 k_\gamma}{a_0\omega}\right)^2}{1-3c_2\left(\frac{b_0 k_\gamma}{a_0\omega}\right)^2}\right] \; , \tag{A-9}$$

$$\left.\frac{\partial k_\tau}{\partial b}\right|_{a_0,b_0} = -\omega \frac{b_0}{a_0}\left(\frac{k_\gamma}{\omega}\right)^2 \frac{1}{\sqrt{1-\left(\frac{b_0 k_\gamma}{a_0\omega}\right)^2}} \approx -\omega \frac{a_0}{b_0}\left(\frac{b_0 k_\gamma}{a_0\omega}\right)^2 \; . \tag{A-10}$$

Therefore, the pseudo-screen equation becomes

$$k_\tau \approx k_{\tau 0} + \omega\,(a - a_0) + \omega \frac{a_0 \left[c_1 \left(\frac{a}{a_0} - 1\right) - \left(\frac{b}{b_0} - 1\right)\right] \left(\frac{b_0}{a_0}\right)^2 \left(\frac{k_\gamma}{\omega}\right)^2}{1 - 3c_2 \left(\frac{b_0}{a_0}\right)^2 \left(\frac{k_\gamma}{\omega}\right)^2} \,. \tag{A-11}$$

If we make the notations

$$\nu = a_0 \left[c_1 \left(\frac{a}{a_0} - 1\right) - \left(\frac{b}{b_0} - 1\right)\right] \left(\frac{b_0}{a_0}\right)^2 \tag{A-12}$$

$$\mu = 1 \tag{A-13}$$

$$\rho = 3c_2 \left(\frac{b_0}{a_0}\right)^2 \tag{A-14}$$

we obtain the mixed-domain pseudo-screen solution to the one-way wave equation in Riemannian coordinates:

$$k_\tau \approx k_{\tau 0} + \omega\,(a - a_0) + \omega \frac{\nu \left(\frac{k_\gamma}{\omega}\right)^2}{\mu - \rho \left(\frac{k_\gamma}{\omega}\right)^2} \,. \tag{A-15}$$

MIXED DOMAIN — FOURIER FINITE-DIFFERENCES

The pseudo-screen solution to equation (13) derives from a fourth-order expansion of the square-root around (a_0, b_0) and (a, b):

$$k_\tau \approx \omega a \left[1 + \frac{1}{2}\left(\frac{b k_\gamma}{a\omega}\right)^2 + \frac{1}{8}\left(\frac{b k_\gamma}{a\omega}\right)^4\right] \,, \tag{A-16}$$

$$k_{\tau 0} \approx \omega a_0 \left[1 + \frac{1}{2}\left(\frac{b_0 k_\gamma}{a_0\omega}\right)^2 + \frac{1}{8}\left(\frac{b_0 k_\gamma}{a_0\omega}\right)^4\right] \,. \tag{A-17}$$

If we subtract equations (A-16) and (A-17), we obtain the following expression for the wavenumber along the extrapolation direction k_τ:

$$\begin{aligned} k_\tau \approx k_{\tau 0} + \omega\,(a - a_0) &+ \frac{1}{2}\omega \left[a \left(\frac{b}{a}\right)^2 - a_0 \left(\frac{b_0}{a_0}\right)^2\right] \left(\frac{k_\gamma}{\omega}\right)^2 \\ &+ \frac{1}{8}\omega \left[a \left(\frac{b}{a}\right)^4 - a_0 \left(\frac{b_0}{a_0}\right)^4\right] \left(\frac{k_\gamma}{\omega}\right)^4 \,. \end{aligned} \tag{A-18}$$

We can make the notations

$$\delta_1 = a \left(\frac{b}{a}\right)^2 - a_0 \left(\frac{b_0}{a_0}\right)^2 \,, \tag{A-19}$$

$$\delta_2 = a \left(\frac{b}{a}\right)^4 - a_0 \left(\frac{b_0}{a_0}\right)^4 \,, \tag{A-20}$$

therefore equation (A-18) can be written as

$$k_\tau = k_{\tau 0} + \omega\,(a - a_0) + \frac{1}{2}\omega\delta_1\left(\frac{k_\gamma}{\omega}\right)^2 + \frac{1}{8}\omega\delta_2\left(\frac{k_\gamma}{\omega}\right)^4 . \tag{A-21}$$

Using the approximation

$$\frac{1}{2}\delta_1 u^2 + \frac{1}{8}\delta_2 u^4 \approx \frac{\frac{1}{2}\delta_1^2 u^2}{\delta_1 - \frac{1}{4}\delta_2 u^2} , \tag{A-22}$$

we can write

$$k_\tau = k_{\tau 0} + \omega\,(a - a_0) + \omega\frac{\frac{1}{2}\delta_1^2\left(\frac{k_\gamma}{\omega}\right)^2}{\delta_1 - \frac{1}{4}\delta_2\left(\frac{k_\gamma}{\omega}\right)^2} . \tag{A-23}$$

If we make the notations

$$\nu = \frac{1}{2}\delta_1^2 , \tag{A-24}$$

$$\mu = \delta_1 , \tag{A-25}$$

$$\rho = \frac{1}{4}\delta_2 , \tag{A-26}$$

we obtain the mixed-domain Fourier finite-differences solution to the one-way wave equation in Riemannian coordinates:

$$k_\tau \approx k_{\tau 0} + \omega\,(a - a_0) + \omega\frac{\nu\left(\frac{k_\gamma}{\omega}\right)^2}{\mu - \rho\left(\frac{k_\gamma}{\omega}\right)^2} . \tag{A-27}$$

REFERENCES

Biondi, B., 2002, Stable wide-angle Fourier finite-difference downward extrapolation of 3-D wavefields: Geophysics, **67**, 872–882.

Claerbout, J., 1998, Multidimensional recursive filters via a helix: Geophysics, **63**, 1532–1541.

Claerbout, J. F., 1985, Imaging the Earth's interior: Blackwell Scientific Publications.

Courant, R., and D. Hilbert, 1989, Methods of mathematical physics: John Wiley & Sons.

Hale, D., 1991, Stable explicit depth extrapolation of seismic wavefields: Geophysics, **56**, 1770–1777.

Huang, L. Y., M. C. Fehler, and R. S. Wu, 1999, Extended local Born Fourier migration method: Geophysics, **64**, 1524–1534.

Rickett, J., J. Claerbout, and S. B. Fomel, 1998, Implicit 3-D depth migration by wavefield extrapolation with helical boundary conditions: 68th Ann. Internat. Mtg, Soc. of Expl. Geophys., 1124–1127.

Ristow, D., and T. Ruhl, 1994, Fourier finite-difference migration: Geophysics, **59**, 1882–1893.

———, 1997, 3-D implicit finite-difference migration by multiway splitting: Geophysics, **62**, 554–567.

Sava, P., and S. Fomel, 2005, Seismic imaging using Riemannian wavefield extrapolation: Geophysics, **70**, T45–T56.

———, 2006, Imaging overturning reflections by Riemannian wavefield extrapolation: Journal of Seismic Exploration, **15**, 209–223.

Shragge, J., 2007, Non-linear Riemannian wavefield extrapolation: Geophysics, submitted for publication.

Shragge, J., and P. Sava, 2005, Wave-equation migration from topography: 75th Ann. Internat. Mtg., Expanded Abstracts, Soc. of Expl. Geophys., 1842–1845.

Stoffa, P. L., J. T. Fokkema, R. M. de Luna Freire, and W. P. Kessinger, 1990, Split-step Fourier migration: Geophysics, **55**, 410–421.

Versteeg, R., 1994, The Marmousi experience: Velocity model determination on a synthetic complex data set: The Leading Edge, **13**, 927–936.